

# EUROPEAN ORGANIZATION FOR NUCLEAR RESEARCH

## Addendum to the IS608 Proposal to the ISOLDE and Neutron Time-of-Flight Committee

### Shape-coexistence and shape-evolution studies for bismuth isotopes by in-source laser spectroscopy

10.01.2017

A. N. Andreyev<sup>1,2</sup>, A. E. Barzakh<sup>3</sup>, N. Althubiti<sup>4</sup>, B. Andel<sup>5</sup>, S. Antalic<sup>5</sup>, J. Billowes<sup>4</sup>, M. Bissell<sup>4</sup>, , K. Chrysalidis<sup>6,7</sup>, T. E. Cocolios<sup>8</sup>, J. Cubiss<sup>1</sup>, D. Doherty<sup>1</sup>, K. Dockx<sup>8</sup>, G. J. Farooq-Smith<sup>8</sup>, D. Fedorov<sup>3</sup>, V. Fedosseev<sup>6</sup>, R. Harding<sup>1</sup>, M. Huyse<sup>8</sup>, P. Larmonier<sup>6</sup>, B.A. Marsh<sup>6</sup>, P. Molkanov<sup>3</sup>, K. Nishio<sup>2</sup>, C. Raison<sup>1</sup>, R.E. Rossel<sup>6</sup>, S. Rothe<sup>6</sup>, C. Seiffert<sup>6</sup>, M. Seliverstov<sup>3</sup>, S.Sels<sup>8</sup>, I. Tsekanovich<sup>9</sup>, P. Van den Bergh<sup>8</sup>, P. Van Duppen<sup>8</sup>, K. Wendt<sup>7</sup>, H. De Witte<sup>8</sup>

<sup>1</sup>University of York, York, UK

<sup>2</sup>Advanced Science Research Center, JAERI, Tokai-mura, Ibaraki, Japan

<sup>3</sup>Petersburg Nuclear Physics Institute, Gatchina, Russia

<sup>4</sup>University of Manchester, UK

<sup>5</sup>Comenius University, Bratislava, Slovakia

<sup>6</sup>CERN, Geneva, Switzerland

<sup>7</sup>Johannes Gutenberg-University, Mainz, Germany

<sup>8</sup>KU Leuven, IKS, Belgium

<sup>9</sup>CENGB, Bordeaux, France

Spokespersons: Andrei Andreyev (University of York) [Andrei.Andreyev@york.ac.uk]  
Anatoly Barzakh (PNPI, Gatchina) [barzakh@mail.ru]  
Piet Van Duppen (IKS) [Piet.VanDuppen@fys.kuleuven.be]  
Local contact: Bruce Marsh – [bruce.marsh@cern.ch]

### Abstract

In 2016, a successful in-source laser spectroscopy campaign for bismuth isotopes was performed by our collaboration (IS608). This Addendum summarizes the preliminary results of these studies and presents the new beam-time request to complete several outstanding goals. The measurements will be performed with the Windmill and by using the new possibilities provided by the ISOLDE Decay Station (IDS)

**Requested shifts:** 13 shifts with a UCx target, with RILIS (+3 already available from previously-approved IS608)



## Introduction

In June-July 2016 a successful investigation of bismuth isotopes (IS608) was performed by our collaboration. 26 shifts of 29 allocated were used. The experiment focused on two main goals: 1) the study of shape-coexistence and shape-evolution phenomena in the long chain of bismuth isotopes ( $^{187-218}\text{Bi}$ ) via isotope shift (IS) and hyperfine structure (hfs) measurements by in-source laser spectroscopy, and 2) beta-delayed fission ( $\beta\text{DF}$ ) studies of two isomerically-separated states in  $^{188}\text{Bi}$ . The experiment greatly benefitted from the availability of two complementary techniques for photo-ion current monitoring: the Windmill (WM) system for short-lived alpha-decaying nuclei and Multi-Reflection Time of Flight Mass Separator (MR-ToF MS) for longer lived isotopes. In September 2016's run, as a part of the IS608 program, hfs measurements for several isotopes in the range of  $^{196-209}\text{Bi}$  were performed by COLLAPS, to clarify the possible existence of isomeric states and to measure the hyperfine anomaly.

This Addendum summarizes the preliminary results of the IS608 run and explains the motivation for a request of 16 shifts to complete several outstanding goals. In addition to the use of WM, for the first time we will make use of the capabilities of IDS to monitor the photo-ion current as a function of laser frequency in an automated scanning procedure.

### Preliminary results of IS608 run

In the 2016 IS608 run, the Bi electromagnetic moments and the changes of the charge radii,  $\delta\langle r^2 \rangle$ , were obtained for  $^{187-191, 194-202, 214-218}\text{Bi}$  (in total, 27 nuclei). The five most interesting findings are as follows:

1. In contrast to previous conclusions on sphericity of the  $9/2^-$  g.s for the light Bi isotopes, based on decay and in-beam studies, *a gradual onset of deformation in the  $9/2^-$  gs of the lightest isotopes was deduced, up to  $\langle \beta^2 \rangle^{1/2} \sim 0.18$  in  $^{187}\text{Bi}$* , see Fig. 1. This effect is exemplified by comparing  $\delta\langle r^2 \rangle$  values for the even-N Pb, Bi and Po isotopes, see Fig. 2, which clearly shows that the radii for the  $9/2^-$  Bi ground state start to deviate from the nearly-spherical trend of the lead isotopes at  $N = 108$  ( $^{191}\text{Bi}$ ) when moving to lower neutron numbers. Moreover, our conclusions are substantiated by the quadrupole moment values (Q) measured in the same IS608 experiment (see Fig. 3).

2. *Large isomer shift, corresponding to more deformed configuration for intruder Bi isomers ( $I^\pi=1/2^+$ ) for  $^{191,199,201}\text{Bi}$*  (Fig. 1), which is the signature of shape coexistence in the corresponding nuclei.

3) *Large shape staggering/coexistence at  $A=188$*  (Fig. 1). This phenomenon is similar to the Hg shape staggering/coexistence and appears at the same N [1] and has nearly the same magnitude (see Fig. 4).

4) *Marked deviation from the presumed linear systematic trend for  $\mu(9/2^-)$  in  $^{215,217}\text{Bi}$*  (Fig. 5).

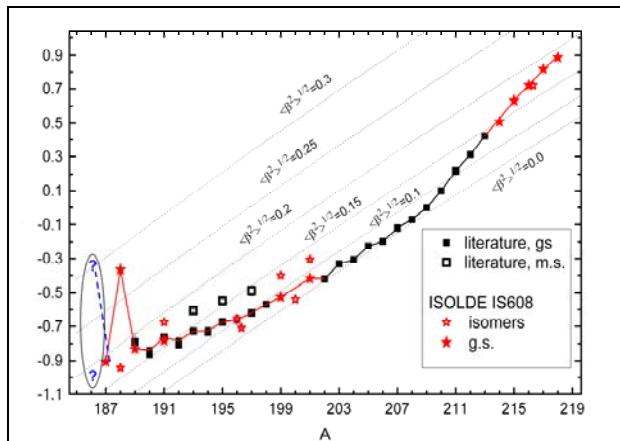


Fig. 1.  $\delta\langle r^2 \rangle$  isotopic dependency for Bi nuclei [2, 3 and IS608].

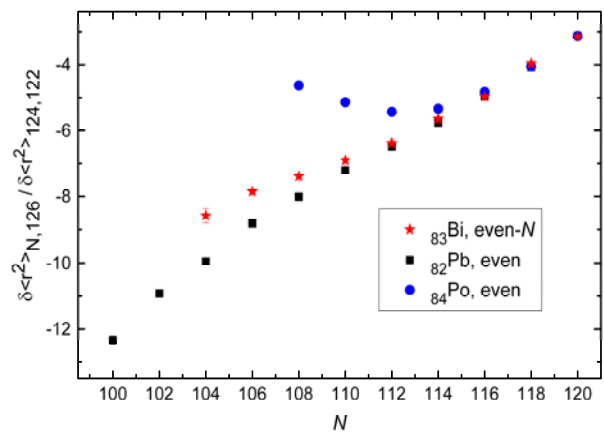


Fig. 2. Comparison of relative  $\delta\langle r^2 \rangle$  for the even-N Pb [4], Bi ( $I^\pi=9/2^-$ ) [3 and IS608], Po [5].

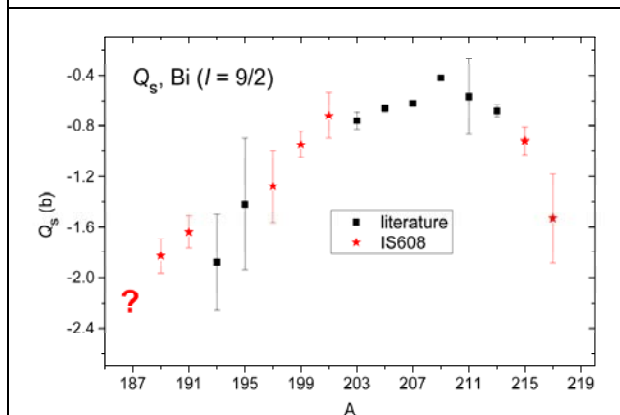


Fig. 3. Quadrupole moments for Bi isotopes with  $I=9/2^-$  [2, 3 and IS608]

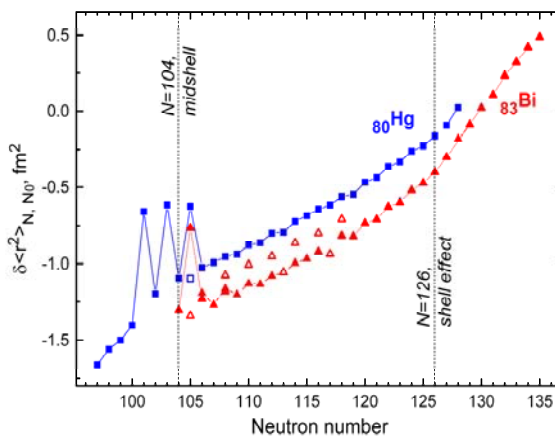


Fig. 4. Comparison of isotopic  $\delta\langle r^2 \rangle$  dependencies for Bi [2, 3 and IS608] and Hg [1 and IS598].

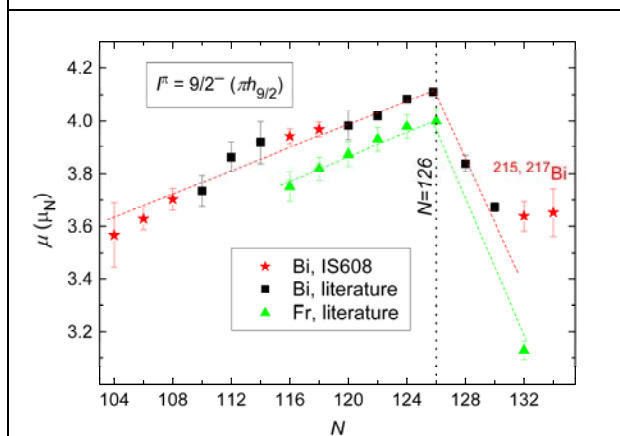


Fig. 5. Magnetic moments for the  $9/2^-$  g. s. of Bi [2, 3, IS608] and Fr [6] isotopes.

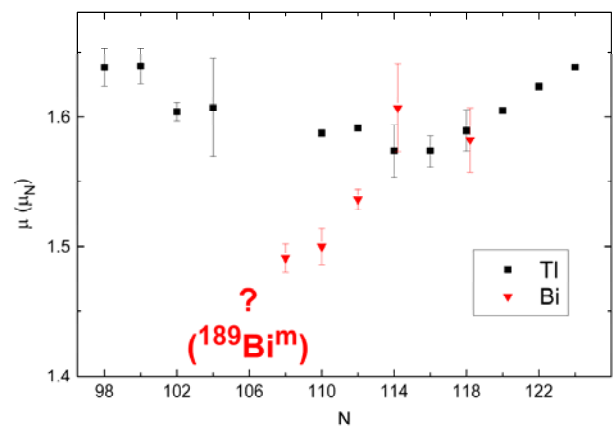


Fig. 6. Magnetic moments for the  $1/2^+$  states of Bi [3, IS608] and Tl [7] isotopes.

5) Fission fragments mass distributions and  $\beta$ DF probabilities for isomerically separated states in  $^{188m1,188m2}\text{Bi}$  were deduced, which enabled us, for the first time, to investigate the spin-dependence of the  $\beta$ DF process and to check theoretical predictions of asymmetrical fission fragment mass-distribution in this region of nuclei. This part of the IS608 is completed.

Some of the above results will be briefly commented upon in the following text, meanwhile in this Addendum we propose to obtain further data to complete the goals of IS608.

### A brief reminder on the underlying physics phenomena in the Bi isotopic chain

While the main goals of the IS608 experiment were described in our original proposal [8], here we will briefly review the underlying physics phenomena and questions, with an emphasis on the need for higher-precision magnetic and quadrupole moment measurements, which became evident from our data, collected in 2016. Fig.7 shows three representative potential energy curves calculated in the Hartree-Fock-Bogoliubov approach with Gogny forces [9] (similar conclusions can be derived from P. Moller's PES calculated in the macro-microscopic approach [10]). The general inference from these calculations is that a gradual transition to deformed configurations is expected when moving towards either neutron-deficient or neutron-rich Bi isotopes. Indeed, while for the semi-magic  $^{209}\text{Bi}$  ( $N=126$ ) one can see the dominant spherical minimum, for  $^{189}\text{Bi}$  ( $N=106$ ) an onset of deformation, with clear signatures of the possible oblate-prolate coexistence is predicted. A similar many-minima picture was obtained for the neighbouring  $^{187}, ^{188}\text{Bi}$ , where the competition of at least four minima at oblate/prolate sides takes place. A detailed discussion of specific configurations was provided in [11], based on PES/PPR calculations. By considering the neutron-rich isotopes, calculations predict an onset of prolate deformation from  $^{222}\text{Bi}$  on (see Fig. 7). The observed trends of  $Q$ 's and  $\mu$ 's for  $^{215}, ^{217}\text{Bi}$  isotopes ( $N=132, 134$ ; see Figs. 3, 5) may be the first indication of this effect. Furthermore, one should keep in mind that, near  $N=132$ , the octupole degree of freedom may begin to influence the structure of the nuclei, as has already been observed for Fr-Rn isotones.

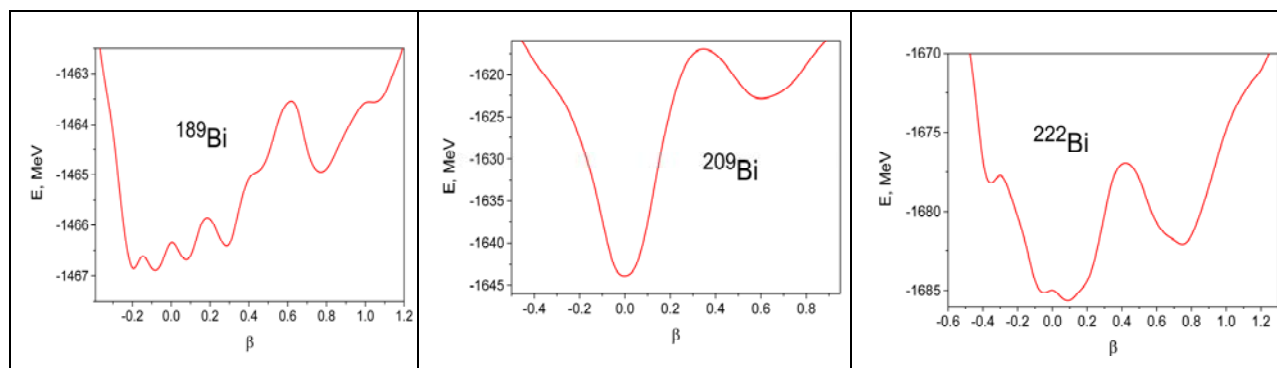


Fig 7. Potential energy curves for  $^{189}, ^{209}, ^{222}\text{Bi}$  calculated in HFB approach with Gogny forces D1S [9].

Therefore, apart from charge radii data, accurate measurements of  $\mu$  and  $Q$ , which are possible with our technique, may elucidate the specific configurations, their mixing and evolution of deformation both on the neutron-deficient and neutron-rich sides.

## Proposed measurements

1. **Quadrupole moment measurements for  $^{187,188m1,188m2,193,195}\text{Bi}$ .** The observed large radius staggering at  $^{188}\text{Bi}$  could be interpreted in the same way as similar staggering at  $^{181-185}\text{Hg}$  (see Fig. 4). Namely, the g.s. of the odd-N  $^{181, 183, 185}\text{Hg}$ -isotopes are believed to be strongly prolate deformed, whereas adjacent even-N isotopes remain weakly oblate deformed. Measurements of the quadrupole moments are needed to support this interpretation. However, in 2016 we did not succeed in measuring the quadrupole moments for  $^{187, 188m1, 188m2}\text{Bi}$  nuclei because an increased laser power had to be used to compensate for the lower production rate. Power broadening therefore prevented an accurate Q-value extraction (with 10% uncertainty achieved for heavier isotopes, see Fig. 3).

From the 2016 run, we conclude that, with a reduced laser power to avoid power broadening, the duration of a laser scan should be increased by a factor of two. Correspondingly we need 1.5 shifts for  $^{188}\text{Bi}$  measurement and 2.5 shifts for  $^{187}\text{Bi}$ .

We also propose to re-measure the Q-values for  $^{193,195}\text{Bi}^g$  during using the capabilities of the IDS (0.5 shift for each isotope). These Q-values are currently only known with a precision of  $\sim 30\text{-}40\%$  [3].

2. **IS/hfs measurements for  $^{189}\text{Bi}^m$  ( $T_{1/2}=5$  ms;  $I=1/2$ ) and  $^{203}\text{Bi}^m$  ( $T_{1/2}=305$  ms;  $I=1/2$ ).** The data for the  $^{189}\text{Bi}^m$  intruder isomer are of importance for understanding the shape coexistence phenomena in this region. As shown by potential-energy surface and particle-rotor calculations [11], the coupling the  $\pi 3s_{1/2}$  proton to the coexisting  $0^+$  states in the lead core should result in occurrence of two closely-spaced (oblate-prolate)  $1/2^+$  states. This phenomenon has been suggested to occur starting from the heavier Bi isotopes  $A < 190$  (see [11] for details). An experimental signature is observed from the IS608 data (Fig. 6) where it can be noticed that the  $\mu(1/2^+)$  for Bi intruder isomers starts to deviate from the “spherical” Tl trend at  $N < 110$ . A measurement of  $\mu(^{189}\text{Bi}^m)$  would be crucial in supporting/rejecting this interpretation. The yield of  $^{189}\text{Bi}^m$  may be estimated taking into account the isomer ratio for  $1/2$  and  $9/2$  states production, the observed yield for  $^{189}\text{Bi}^{g.s.}$  ( $T_{1/2}=0.66$  s;  $Y(^{189}\text{Bi}^{g.s.})=3 \times 10^2 1/\mu\text{C}$ ) and decay losses for the short-lived  $^{189}\text{Bi}^m$ :  $Y(^{189}\text{Bi}^m) \sim 1 1/\mu\text{C}$ . As the result, a hfs spectrum with 20 counts in the maximum could be obtained in a 9-hours scan. To obtain 2 hfs-spectra 2.5 shifts are therefore needed.

To complete the systematics of the intruder isomer shift and  $\mu(1/2^+)$  evolution it is of importance to measure the IS/hfs also for the heaviest attainable intruder isomer,  $^{203}\text{Bi}^m$ . The yield,  $Y(^{203}\text{Bi}^m) \sim 2 \times 10^6 1/\mu\text{C}$ , was measured previously, see [12].  $^{203}\text{Bi}^m$  has intense IT  $\gamma$  lines and will be readily measurable with the aid of IDS (0.5 shift).

3.  **$^{217, 219}\text{Bi}$ .** During the IS608 run an unexpected behavior of  $\mu(9/2^-)$  was observed (see Fig. 5). While on the neutron-deficient side the trends of  $\mu$  for Bi and Fr follow each other closely, a clear deviation of the  $\mu$ 's for  $^{215, 217}\text{Bi}$  from the supposed systematics (see straight lines in Fig. 5) was observed. Therefore, we propose to trace the behavior of  $\mu(9/2^-)$  to more neutron-rich isotopes and to decrease uncertainties for  $^{217}\text{Bi}$ . The yield of  $^{218}\text{Bi}$  was estimated in our 2016 experiment:  $\sim 3 \times 10^2 1/\mu\text{C}$ . Thus the yield of  $^{217}\text{Bi}$  will be  $> 3 \times 10^2 1/\mu\text{C}$  and 0.5 shift will be sufficient for two scans. With a conservative estimation of the decrease of the yield when going from  $^{218}\text{Bi}$  to  $^{219}\text{Bi}$  (10 times) one can estimate the required beam-time request for  $^{219}\text{Bi}$  as 1.5 shifts (2 scans).

**4. High-spin isomers for the N>126 Bi isotopes.** We propose to study five long-lived high-spin Bi isomers which are known in this region (with the tentative configuration assignment):  $^{212}\text{Bi}^{m1} (\pi h_{9/2} \otimes \nu g_{9/2})_{8,9}$ ,  $^{212}\text{Bi}^{m2} [\pi h_{9/2} \otimes ((\nu g_{9/2})^2 \otimes \nu i_{11/2})]_{18}$ ,  $^{213}\text{Bi}^m$   $[\pi h_{9/2} \otimes (\nu g_{9/2} \otimes \nu i_{11/2})]_{25/2}$ ,  $^{214}\text{Bi}^m$  (configuration unknown) and  $^{215}\text{Bi}^m$   $[\pi h_{9/2} \otimes (\nu g_{9/2} \otimes \nu i_{11/2})]_{25/2-29/2}$  [13, 14]. Apart from valuable information for configuration assignment which will be obtained through magnetic moment measurements, the investigation of charge radii of these isomers will shed the light on the nature of the well-known and yet poorly understood shell-effect in the charge radii trend (see the kink in  $\delta\langle r^2 \rangle$  at N=126 in Figs. 1, 4). According to the Hartree-Fock calculations in [15] the value of this kink is critically dependent on the occupancy of the neutron  $\nu i_{11/2}$  shell. This occupancy is dramatically changed for the high-spin Bi isomers in comparison with the corresponding ground states. Therefore, one expects a noticeable change in the  $\delta\langle r^2 \rangle$  behavior for these isomers provided the interpretation of [15] is valid. Note, that previously the laser spectroscopy study of the high-spin Po isomers at N>126 was proposed with the reference to the same shell-effect model [16].

For neutron rich Bi isotopes the well-known problem of the huge surface ionized Fr (Ra) background exists.  $^{215}\text{Bi}$  was successfully studied at ISOLDE on tape station applying pulsed-release technique [14]. This work reliably proves the possibility of using strong gamma lines following  $\beta$  decay or/and IT of mentioned Bi isotopes/isomers as a monitor of the photo-ion current at IDS. The same technique may be used for  $^{214}\text{Bi}^m$ . For  $^{212}\text{Bi}^{m1, m2}$ ,  $^{213}\text{Bi}^m$  isomers high-energy  $\alpha$  lines following their  $\beta$  decay may be used ( $E_\alpha=10180$  keV,  $^{212}\text{Bi}^{m1}$ ;  $E_\alpha=11660$  keV,  $^{212}\text{Bi}^{m2}$ ;  $E_\alpha=8376$  keV,  $^{213}\text{Bi}^m$ ). These  $\alpha$  lines lie far from the background  $^{212}\text{Fr}$  (6100—6400 keV),  $^{213}\text{Fr}$  (6775 keV) and will not be hidden by these background lines. Taking into account the unknown position of the hfs component “rough” scan with larger frequency step for search of these position is needed for all isomers. Thus, we estimate the needed beam time as 1 shift for each isomer, thus 5 shifts in total.

### Technique

Apart from the use of WM (for light,  $\alpha$ -decaying isotopes) we will exploit for the first time IDS assisted scanning. At present the synchronization of IDS with RILIS is being developed, and should be ready by Spring 2017. The singles  $\gamma$ -ray efficiency of IDS in the range of 200-400 keV (where we expect the most intense decays) is  $\sim 7-9\%$ , thus a total efficiency of 20-30% can be reached for decays involving high  $\gamma$ -ray multiplicity. This enables us to make IS/hfs measurements at the yields  $\sim 10^2-10^1$  1/ $\mu\text{C}$ . At the same time the use of IDS now opens up further possibilities for detailed nuclear spectroscopy studies via  $\beta/\gamma$  spectroscopy (especially for poorly studied high-spin isomers at N>126).

In Table 1 the list of isotopes to be studied with the corresponding beam-time request are presented. Yields were estimated using the observed during the IS608 run count rates with known/extrapolated isomer ratios.

Table 1. Estimated beam-time request for Bi nuclei (see text for details).

A	I	$T_{1/2}$ , s	Yield, 1/s/ $\mu\text{C}$	Method of measurement	time, shifts
219	(9/2)	22	$>3 \times 10^1$	IDS	1.5
217	(9/2)	98.5	$>3 \times 10^2$	IDS	0.5
215m	(29/2–25/2)	36.9	$>1 \times 10^3$	IDS	1

214m	?	>93	$>1 \times 10^3$	IDS	1
213m	(25/2)	>168	$>1 \times 10^3$	IDS	1
212m1	(18)	420	$>1 \times 10^3$	IDS	1
212m2	(8.9)	1500	$>1 \times 10^3$	IDS	1
203m	1/2	0.305	$1.9 \times 10^6$	IDS	0.5
195	(9/2)	183	$1.4 \times 10^7$	IDS	0.5
193	(9/2)	63.6	$3 \times 10^6$	IDS	0.5
189m	(1/2)	0.005	1	WM	2.5
188m1	(3)	0.06	20	WM	1.5
188m2	(10)	0.265	$10^2$	WM	
187g	(9/2)	0.037	0.3	WM	2.5

To summarize, we intend to study IS and hfs of  $^{187, 188, 203m, 212m, 213m, 214m, 215m, 217, 219}\text{Bi}$ . The total beam time request: 15 shifts + 1 shift for the reference measurements, **total 16 shifts**. By accounting for 3 remaining shifts from IS608, the present beam-time request is 13 shifts

### References:

- [1] G. Ulm *et al.*, Z. Phys. A **325**, 247 (1986).
- [2] M. R. Pearson *et al.*, J. Phys. G: Nucl. Part. Phys. **26** (2000) 1829.
- [3] A. Barzakh *et al.*, Phys. Rev. C **94**, 024334 (2016).
- [4] H. De Witte *et al.*, Phys. Rev. Lett. **98**, 112502 (2007); M. Seliverstov *et al.*, Eur. Phys. J., A**41**, 315 (2009).
- [5] T. E. Cocolios *et al.*, Phys. Rev. Lett. **106**, 052203 (2011); M. Seliverstov *et al.*, Phys. Rev. C **89**, 034323, (2014).
- [6] R. P. de Groote *et al.*, PRL **115**, 132501 (2015).
- [7] A. Barzakh *et al.*, in press.
- [8] <http://cds.cern.ch/record/2059118/files/INTC-P-443.pdf>
- [9] S. Hilaire, M. Girod, Hartree-Fock-Bogoliubov results based on the Gogny force, [http://www-phynu.cea.fr/science\\_en\\_ligne/carte\\_potentiels\\_microscopiques](http://www-phynu.cea.fr/science_en_ligne/carte_potentiels_microscopiques)
- [10] P. Möller, A. J. Sierk, R. Bengtsson, H. Sagawa, T. Ichikawa, ADNDT **98** (2012) 149; <https://t2.lanl.gov/nis/data/astro/molnix96/peseps2gamma.html>
- [11] A. N. Andreyev *et al.*, Phys. Rev. C **69**, 054308 (2004).
- [12] ISOLDE yield Database, [http://test-isolde-yields.web.cern.ch/test-isolde-yields/query\\_tgt.htm](http://test-isolde-yields.web.cern.ch/test-isolde-yields/query_tgt.htm)
- [13] L. Chen *et al.*, PRL **110**, 122502 (2013); L. Chen *et al.*, Nuclear Physics A **882** (2012) 71; L. Chen, thesis, Gießen, 2008.
- [14] J. Kurpeta *et al.*, Eur. Phys. J. A **18**, 31 (2003).
- [15] P. M. Goddard, P. D. Stevenson, and A. Rios. Phys. Rev. Lett., **110**, 032503, 2013.
- [16] T. E. Cocolios *et al.*, Addendum to IS456. INTC-P-222-ADD-2: <http://cds.cern.ch/record/1642843/files/?ln=en>.

## Appendix

### DESCRIPTION OF THE PROPOSED EXPERIMENT

The experimental setup comprises a Windmill system with 2-4 Si detectors inside, and 1-2 Ge detectors outside. WM system was successfully used in the runs IS387, IS407, IS456, IS466, I-086 and IS534, therefore solid understanding of all possible hazards is available. We will use also usual IDS settings/detectors with the standard calibration sources.

Part of the Choose an item.	Availability	Design and manufacturing
Windmill and IDS	<input checked="" type="checkbox"/> Existing	<input checked="" type="checkbox"/> To be used without any modification

### HAZARDS GENERATED BY THE EXPERIMENT

Hazards named in the document relevant for the fixed IDS installation.

Additional hazards:

Hazards	Windmill	IDS
<b>Thermodynamic and fluidic</b>		
Pressure	-	
Vacuum	Standard ISOLDE vacuum	
Temperature		
Heat transfer		
Thermal properties of materials		
Cryogenic fluid	LN2, 2 Bar, 150 l	
<b>Electrical and electromagnetic</b>		
Electricity	Standard power supplies	
Static electricity		
Magnetic field		
Batteries	<input type="checkbox"/>	
Capacitors	<input type="checkbox"/>	
Ionizing radiation		
Target material [C-foils]	The C foils, where the radioactive samples are implanted, are very fragile. Should they break upon opening the Windmill, the pieces are so light that they would become airborne. Great care must be taken when opening the system and removing them (slow pumping/venting protective equipment: facial mask).	
Beam particle type (e, p, ions, etc)		
Beam intensity		
Beam energy		
Cooling liquids		
Gases		
Calibration sources:	<input type="checkbox"/>	

• Open source	<input type="checkbox"/>	
• Sealed source	<input type="checkbox"/>	
• Isotope	<sup>239</sup> Pu, <sup>241</sup> Am, <sup>244</sup> Cm	
• Activity	1 kBq each	
Use of activated material:		
• Description	<input type="checkbox"/>	
• Dose rate on contact and in 10 cm distance		
• Isotope		
• Activity		
<b>Non-ionizing radiation</b>		
Laser	Standard RILIS operation	
UV light		
Microwaves (300MHz-30 GHz)		
Radiofrequency (1-300MHz)		
<b>Chemical</b>		
Toxic	Pb shielding, 30-40 bricks	
Harmful		
CMR (carcinogens, mutagens and substances toxic to reproduction)		
Corrosive		
Irritant		
Flammable		
Oxidizing		
Explosiveness		
Asphyxiant		
Dangerous for the environment		
<b>Mechanical</b>		
Physical impact or mechanical energy (moving parts)	The chamber is heavy and needs to be handled with care during installation/removing	
Mechanical properties (Sharp, rough, slippery)		
Vibration		
Vehicles and Means of Transport		
Frequency		
Intensity		
Confined spaces		
High workplaces		
Access to high workplaces		
Obstructions in passageways		
Manual handling		
Poor ergonomics		

## 0.1 Hazard identification

3.2 Average electrical power requirements (excluding fixed ISOLDE-installation mentioned above):  
Negligible

